Draft version November 27, 2009
Preprint typeset using LaTeX style emulateapj v. 08/22/09

arXiv:0911.5358v1 [astro-ph.HE] 27 Nov 2009

OPTICAL TRANSIENTS FROM THE UNBOUND DEBRIS OF TIDAL DISRUPTION

Daniel Kasen[1,2] Enrico Ramirez-Ruiz[1]

Draft version November 27, 2009

ABSTRACT

In the tidal disruption of a star by a black hole, roughly half of the stellar mass becomes bound and falls into the black hole, while the other half is ejected at high velocity. Several previous studies have considered the emission resulting from the accretion of bound material; we consider the possibility that the unbound debris may also radiate once it has expanded and become transparent. We show that the gradual energy input from hydrogen recombination compensates for adiabatic loses over significant expansion factors. The opacity also drops dramatically with recombination, and the internal energy can be radiated by means of a cooling-transparency wave propagating from the surface layers inward. The result is a brief optical transient occurring $\sim$ 1 week after disruption and lasting 3-5 days with peak luminosities of $10^{40}-10^{42}$ ergs s^{-1}, depending on the mass of the disrupted star. These recombination powered transients should accompany the x-ray/ultraviolet flare from the accretion of bound material, and so may be a useful signature for discriminating tidal disruption events, especially for lower and intermediate mass black holes.

Subject headings:

1. INTRODUCTION

Stars unfortunate enough to pass too close to a massive black hole are torn apart by tidal gravity forces. In the process, roughly half of the stellar material becomes bound, circularizes, and may eventually accrete onto the black-hole. The other half of the star is ejected from the system at high differential velocities.

Tidal disruption events offers one means of probing a central black hole in quiescent galaxies. The dominant observational signature should be a bright x-ray flare powered by accretion of bound material onto the black hole (Rees 1988; Ulmer 1999; Ramirez-Ruiz & Rosswog 2009). Candidate disruption flares have been detected in x-ray/ultraviolet surveys (Donley et al. 2002; Gezari et al. 2006; Esquej et al. 2007) in some case with counterpart emission in the optical (Gezari et al. 2009). The light curves decline as power laws with luminosities comparable to the Eddington luminosity for $10^6-10^7\ M_\odot$ black holes. Nevertheless, it can be difficult to uniquely identify these flares as tidal disruption events as opposed to other forms of nuclear activity.

It is therefore useful to determine additional discriminating signatures of tidal disruption events. A few possibilities have been suggested. For deeply penetrating orbits, strong tidal compression perpendicular to the orbital plane leads to the formation of shocks, which breakout out in short ($\sim$ 100 sec) but bright ($L \sim 10^{43}$ ergs s^{-1}) x-ray bursts (Kobayashi et al. 2004; Brassart & Luminet 2008; Guillochon et al. 2008). Later on, streams of material falling onto the black hole may undergo collisions producing short UV flares of luminosity $10^{40}-10^{41}$ ergs s^{-1} (Cannizzo et al. 1990; Kim et al. 1999). In addition, the x-ray/UV luminosity from accretion may be absorbed and reprocessed by the unbound debris into optical emission, leading to optical luminosities of $\sim 10^{40}$ ergs s^{-1} (Bogdanović et al. 2004; Strubbe & Quataert 2009). If a substantial fraction of the accreting material is blown in a wind, the optical radiation escaping from this outflow may be much brighter, $10^{42}-10^{43}$ ergs s^{-1} (Strubbe & Quataert 2009). Optical emission is of particular interest, as observational surveys are typically most sensitive at these wavelength.

Little attention has been given to emission from the unbound debris of disruption. This material, which expands differentially with velocities $\sim 10^4$ km s^{-1} in some ways resembles a supernova remnant, though usually lacking any radioactive isotopes to power the light curve. While the initial internal energy of the star can be fairly significant ($E_{\rm int} \sim 10^{48}$ ergs), most of it will be lost to adiabatic expansion before the ejecta becomes sufficiently transparent to radiate. For an ideal gas with adiabatic index $\gamma = 5/3$, the energy and temperature evolve adiabatically as $E \propto \rho^{(\gamma-1)} \propto \rho^{2/3}$. A decline in density by at least a factor of $\sim 10^9$ is required before the debris might become translucent, at which point the internal energy and temperature will have decreased by a factor $\sim 10^6$. Hence the apparent lack of interest in diffusive thermal emission from the unbound remnants of tidal disruption.

There is, however, another important energy reservoir of the debris – ionization energy, which amounts to $\sim 10^{46}$ ergs per solar mass of ionized hydrogen and is not subject to adiabatic degradation. When recombination eventually sets in at temperatures $T_i \sim 10^4$ K, the energy released per atom ϵ_i is an order of magnitude greater than the mean thermal energy, $\epsilon_i/kT_i \approx 15$. Recombination is therefore a gradual process, steadily inputting energy to maintain the gas temperature near T_i. The thermodynamic evolution is described by $E \propto \rho^{(\gamma_3-1)}$ where γ_3 is the third generalized adiabatic index, now a function of density and temperature. In the region of partial ionization $\gamma_3 - 1 \approx 2kT/\epsilon_i \approx 0.1$ (see §3) so that the energy decline is indeed gradual.

When the effects of ionization are included, the debris can expand by a much larger factor, and reach much

---

[1] University of California, Santa Cruz
[2] Hubble Fellow

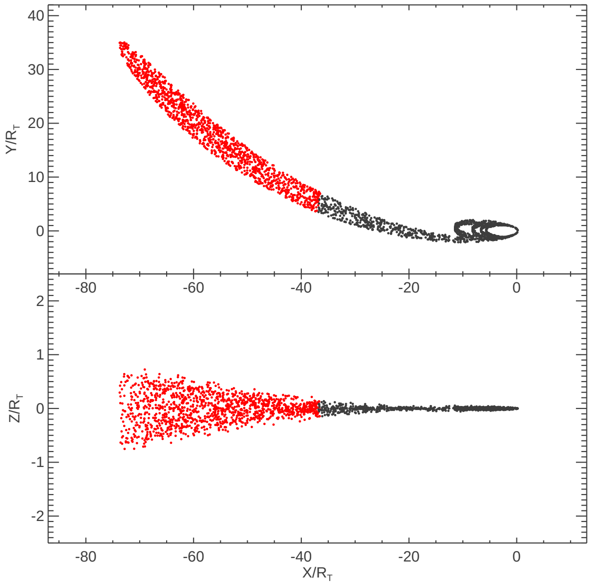

FIG. 1.— Geometrical distribution of the debris (2 days after pericenter passage) for a $\beta = 5$ tidal disruption of a solar type star by a $10^6\ M_\odot$ black hole. The location of individual points was determined by following the collisionless orbits of particles under the gravity of the black hole, starting from a pancake configuration at pericenter. The top panel shows a slice through the orbital plane, while the bottom panel shows the distribution perpendicular to the orbital plane (note the vertical axis of the bottom panel is zoomed by a factor of 10). Black points denote bound material and red points unbound material.

lower densities, before the internal energy is depleted. When near neutrality is reached, the opacity also drops sharply due to the elimination of electron scattering. It may be possible for radiation to escape at this time, taking the form of a cooling-transparency wave that propagates from the surface inwards. The escape of photons will be aided by the aspherical geometry of the debris, which has been stretched by tidal forces into a thin stream, with lower optical depth along the direction perpendicular to the orbital plane

It is therefore plausible that the unbound debris of tidal disruptions gives rise to a brief optical transient powered primarily by the energy tapped from recombination. We call such an event a recombination transient (RT). The light curves, even if they are dim, might be relevant for upcoming synoptic optical surveys which will probe for the first time extra-galactic transients with luminosities between classical novae ($M_R > -10$ mag) and supernovae ($M_R < -14$ mag). Here we elaborate on the basic physical ideas and make approximate predictions of the light curves.

2. THE DEBRIS OF TIDAL DISRUPTION

The dynamics of tidal disruption have been widely studied, both analytically and numerically (e.g., Rees 1988; Carter & Luminet 1983; Kochanek 1994; Brassart & Luminet 2008; Lodato et al. 2009; Guillochon et al. 2008; Ramirez-Ruiz & Rosswog 2009). Disruption occurs when a star passes within the tidal radius $R_T = R_\star (M_{\rm bh}/M_\star)^{1/3}$, where $M_{\rm bh}$ is the black hole mass, and $M_\star$ and $R_\star$ the stellar mass and radius. The penetration factor $\beta = R_T/R_p$ describes the depth of the encounter, where R_p is the radius at pericenter. The velocity at pericenter is $v_p = (2GM_{\rm bh}/R_p)^{1/2}$ or

$$v_p \approx 6\times 10^4\ \beta^{1/2}\ m_6^{1/3} {m_\star}^{1/6} {r_\star}^{-1/2}\ {\rm km\ s^{-1}} \qquad (1)$$

where $m_6 = M_{\rm bh}/(10^6 M_\odot)$, $m_\star = M_\star/M_\odot$, and $r_\star = R_\star/R_\odot$. Because the initial velocity of the star at infinity (~ 100 km s^{-1}) is much less than v_p, it is assumed to approach on an essentially parabolic orbit.

Within R_T, the self-gravity of the star becomes subdominant. Material on the far side of the star, being more distant to to the black hole by $R_\star$, possesses an excess specific energy relative to the center of mass, $\Delta\epsilon = GM_{\rm bh}R_\star/R_p^2$. This material becomes unbound with an expansion velocity at infinity $v_\infty = (2\Delta\epsilon)^{1/2}$ or

$$v_\infty \approx 6\times 10^3\ \beta\ m_6^{1/6} {m_\star}^{1/3} {r_\star}^{-1/2}\ {\rm km\ s^{-1}} \qquad (2)$$

The half of the star nearer to the black hole, with specific energy $-\Delta\epsilon$, becomes bound and eventually may accrete onto the black hole.

The unbound material is ejected from the system on hyperbolic orbits, and the debris elongates into a thin stream (Khokhlov & Melia 1996; Kochanek 1994; Rosswog et al. 2009). We describe the final geometry with the parameters R_o, R_t, and R_z which denote, respectively, the spatial extant of the debris in the orbital direction, the transverse direction within the orbital plane, and the direction perpendicular to the orbital plane. The thickness of the stream within the orbital plane is related to the difference in specific energy between the leading and trailing edges of the star as it approaches pericenter, $\Delta\epsilon_t = GM_{\rm bh}{R_\star}^2/R_p^3$. Comparing the corresponding velocity at infinity $v_t = (2\Delta\epsilon_t)^{1/2}$ to v_∞ provides a estimate of the axis ratio $E_t = R_o/R_t$.

$$E_t \approx v_\infty/v_t \approx 10\ \beta^{-1/2}(m_6/m_\star)^{1/6} \qquad (3)$$

In the dimension perpendicular to the orbital plane (the z-direction) tidal forces compress the star into a pancake (Guillochon et al. 2008). The compression raises the central density by a factor proportional to β^3 (Carter & Luminet 1983), with a corresponding adiabatic increase in temperature of $T \propto \rho^{(\gamma-1)} \propto \beta^2$. Eventually the star rebounds under the increased central pressure. For deep penetrations ($\beta \gtrsim 3$), shocks form and propagate outward in the z-direction. The temperature of the shocked material will be of order the virial temperature

$$T_\star \approx \beta^2 \frac{GM_\star \mu m_p}{R_\star k_b} \approx 1\times 10^7\ \beta^2 m_\star {r_\star}^{-1}\ {\rm K} \qquad (4)$$

where $\mu = 0.5$ is the mean particle mass of ionized hydrogen. The velocity in the z-direction of the shocked material will be of order

$$v_z \approx (3kT_\star/\mu m_p)^{1/2} \approx 600\ \beta\ {m_\star}^{1/2}{r_\star}^{-1/2}\ {\rm km\ s^{-1}} \qquad (5)$$

Comparable shock velocities can be seen in the hydrodynamical calculations of Brassart & Luminet (2008). This z-velocity serves to increase final the spatial extent of the unbound debris in the z-direction. The orbital plane of a gas element with non-zero z-velocity at pericenter will be inclined to the plane of the stellar orbit by an angle $\arcsin(v_z/v_p)$. The axis ratio of the debris in the direction perpendicular to the orbital plane $E_z = R_o/R_z$ is then approximately

$$E_z \approx v_p/v_z = 100\, \beta^{-1/2}(m_6/m_\star)^{1/3} \tag{6}$$

We can model approximately the final shape of the unbound debris by simply following the orbits of collisionless test particles in the gravitational potential of the black hole, while ignoring self-gravity. For initial conditions at pericenter we take a uniform pancake of radius $R_\odot$ moving in the y-direction with speed v_p and with a z-component of velocity given by Eq. 5. Two days later, the final thin stream geometry (Figure 1) is roughly described by axis ratios of $E_z = 100$ and $E_t = 10$.

The unbound debris eventually enters a homologous phase and the volume scales as $V(t) = {R_\star}^3\zeta^3$ where we define the expansion parameter:

$$\zeta = (R_o R_t R_z)^{1/3}\frac{1}{R_\star} = \frac{v_\infty t}{R_\star}(E_z E_t)^{-1/3} \tag{7}$$

We can also write $\zeta(t) = t/t_e$ where the expansion time is defined

$$\begin{aligned} t_e &= \frac{R_\star}{v_\infty}(E_z E_t)^{1/3} \\ &= 1120\ \beta^{-1} m_6^{-1/6} {m_\star}^{-1/3} {r_\star}^{3/2}\left(\frac{E_z E_t}{1000}\right)^{1/3}\ \text{sec} \end{aligned} \tag{8}$$

Initially, the stellar mass and energy are centrally concentrated, but shocks largely homogenize the density and temperature structures in the vertical direction (Brassart & Luminet 2008; Guillochon et al. 2008; Rosswog et al. 2009). This outward transport of entropy is an important factor in obtaining a bright transient. The total internal energy of the unbound debris after it has rebounded to its original volume will be of order its original value

$$E_{\rm int} = f_E \frac{1}{2}\frac{G{M_\star}^2}{R_\star} \approx 2\times 10^{48}\ f_E {m_\star}^2 {r_\star}^{-1}\ \text{ergs.} \tag{9}$$

where f_E is a constant of order unity. By comparison, the total kinetic energy at infinity of the unbound debris is of order $E_{\rm KE} = 1/4 M_\star v_\infty^2 \approx \beta^2 2\times 10^{50}$ ergs. The ratio of internal to kinetic energy is initially $E_{\rm int}/E_{\rm KE} \approx 10^{-2}\beta^{-2} \ll 1$, which can be contrasted with that of shock driven Type II supernovae, $E_{\rm int}/E_{\rm KE} \approx 1$. The difference in initial entropy results in a distinct thermodynamic evolution and light curve for the two events.

3. THERMODYNAMIC EVOLUTION

Following disruption, the evolution of the expanding debris follows the thermodynamics of ionizing gases (Krishna Swamy 1961; Mihalas & Weibel Mihalas 1984). Initially the material is extremely optically thick and the evolution essentially adiabatic, $dE = -PdV$, where the pressure is

$$P = (1+\bar{x})\frac{NkT}{V} + \frac{1}{3}aT^4, \tag{10}$$

with N the number of nuclei and V the volume. The mean ionization state is $\bar{x} = \sum_i A_i x_i$, where x_i is the ionization fraction and A_i the abundance fraction of species i. For our purposes, only hydrogen and two ionization states of helium need be considered. The total internal energy is

$$E = \frac{3}{2}(1+\bar{x})NkT + aT^4V + \sum_i N A_i x_i \epsilon_i \tag{11}$$

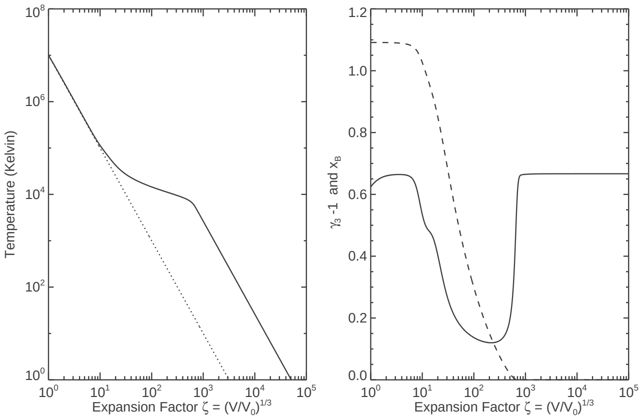

FIG. 2.— Thermodynamic evolution of a parcel of gas with initial temperature $T_0 = 2\times 10^7$ K and density $\rho_0 = 1$ g cm^3. *Left:* Temperature (solid line) as a function of expansion factor in radius. The dashed line shows the $T \propto \zeta^{-2}$ law for a constant $\gamma = 5/3$ gas. The plateau in temperature starting at $\zeta \approx 10$ is due to the energy input from recombination. *Right:* Evolution of the effective adiabatic index $\gamma_3 - 1$ (solid line) and the mean ionization fraction $\bar{x}$ (dotted line) as a function of the expansion factor. In the region of partial ionization, $\gamma_3 - 1 \approx 0.1$.

Excitation energy terms can be ignored. Once the temperature is high enough to excite the atoms the gas will quickly become ionized.

Assuming local thermodynamic equilibrium the ionization state of each species is given by the Saha equation:

$$\frac{x_i}{1-x_i}\frac{\bar{x}}{V} = \frac{c_i}{Z_i}T^{3/2}\exp -\frac{\epsilon_i}{kT} \tag{12}$$

where c_i is a constant, and Z_i is the partition function, which we take to be independent of temperature and density.

From Eq. 11 we have

$$\begin{aligned} dE = NkT \sum A_i dx_i \left[\frac{3}{2} + \frac{\epsilon_i}{kT}\right] + \\ \frac{dT}{T}\left[\frac{3}{2}(1+\bar{x})NkT + 4aT^4V\right] + \frac{dV}{V}aT^4V \end{aligned} \tag{13}$$

while the logarithmic derivative of Eq. 12 gives:

$$\frac{dx_i}{x_i(1-x_i)} + \frac{d\bar{x}}{\bar{x}} - \frac{dV}{V} = \frac{dT}{T}\left[\frac{5}{2} + \frac{\epsilon_i}{kT}\right] \tag{14}$$

Because the ionization energies of hydrogen and helium are fairly well separated, we approximate $d\bar{x} = dx_i$

Combining Eqs. 13, 14, and 10 gives for adiabatic evolution

$$\frac{dT}{T} = (\gamma_3 - 1)\frac{dV}{V} \tag{15}$$

where

$$\gamma_3 = 1 + \frac{(1+\bar{x})(1+4\alpha) + \sum_i A_i \frac{x(1-x)}{(2-x)}(\frac{3}{2}+\frac{\epsilon_i}{kT})}{(1+\bar{x})(\frac{3}{2}+12\alpha) + \sum_i A_i \frac{x(1-x)}{(2-x)}(\frac{3}{2}+\frac{\epsilon_i}{kT})^2} \tag{16}$$

were $\alpha = aT^4V/3NkT(1+\bar{x})$ is the ratio of radiation pressure to gas pressure. The sum here runs over both ionization states of helium, treated independently.

When either the gas or radiation terms dominate, Eq. 16 reduces as expected to $\gamma_3 = 5/3$ or $4/3$, respectively. The terms under the sums, which incorporate the effects of ionization, are zero for $x = 0$ and 1 but maximal in the region of partial ionization of hydrogen. For $x_H \approx 0.6$ we get the smallest values of γ_3

$$(\gamma_3 - 1)_{\rm min} \approx \frac{k_B T}{\epsilon_H}\left[1 + 10\frac{k_b T}{\epsilon_H}(1+\alpha)\right] \approx 0.1\ \left(\frac{T}{10^4\ {\rm K}}\right) \tag{17}$$

where we used the fact that $\epsilon_H/k_B T \approx 15$ for temperatures $T \approx 10^4$ K.

From Eq 17 we can estimate the amount of expansion the debris will undergo before recombination is complete. For an initial temperature of $T = 10^7$ K and density $\rho = 1$ g cm^3, gas energy dominates and one has at first $T \propto \zeta^{-2}$. The debris will expand by a factor $\zeta \approx 10$ before the temperature drops into the regime of recombination at $T \sim 4 \times 10^4$ K. Hydrogen remains partially ionized for only a narrow temperature range, however this occurs over an extended period of time − to reduce T from 4×10^4 K down to 1×10^4 requires additional expansion by a factor $\sim 4^{1/3(\gamma_3 - 1)_{\rm min}} \sim 100$. Thus, for these initial conditions, we anticipate total expansion of $\zeta_R \approx 1000$ before recombination is complete.

Figure 2 shows the thermodynamic evolution of a parcel of gas with the above initial conditions, as determined from a direct numerical integration of Eq. 15. The initial $T \propto \zeta^{-2}$ law plateaus at $\zeta \approx 10$, after which the gradual input of energy from recombination maintains the temperature at a near constant value. As expected, recombination is essentially complete by $\zeta_R \approx 1000$, and the $T \propto \zeta^{-2}$ behavior resumes. Naturally, a higher initial temperature allows for larger expansion factors, but so does a lower density. This is because at lower density recombination occurs at a lower temperature, which implies a lower $\gamma_3 - 1$ in the recombination regime (Eq. 17).

4. OPACITY AND RADIATIVE TRANSFER

After the debris has expanded by a factor $\zeta_R \sim 1000$ and recombined, its internal energy is around 10^{45} ergs per $M_\odot$ of hydrogen. This is ~ 500 times greater than what is predicted for a constant $\gamma = 5/3$ evolution, demonstrating the critical importance of the ionization effects. If the energy can be radiated on the time scale of days, a bright transient may be produced. However, if the debris remains optically thick the energy will lost quickly to expansion in the gas dominated regime.

Radiation will preferentially escape along the z-direction, the shortest dimension with extant $R_z = R_\star \zeta E_z^{-2/3} E_t^{1/3}$. The total optical depth along this direction is $\tau_z = \rho \kappa_R R_z$, or taking an average value for the density

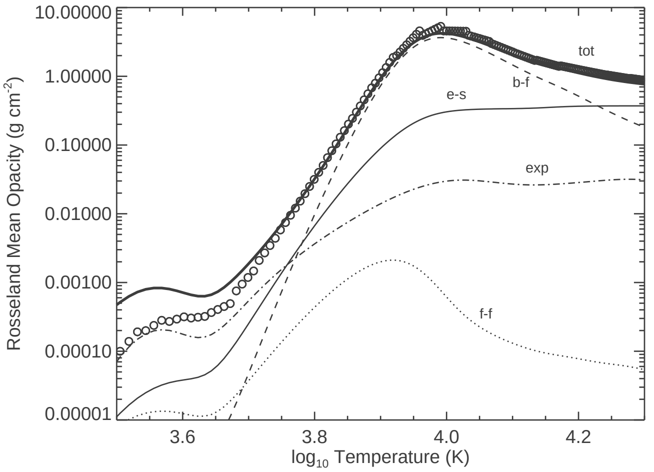

FIG. 3.— Rosseland mean opacity as a function of temperature for solar metallicity material with density $\rho = 10^{-10}$ at a time $t = 5 \times 10^5$ sec. The thick solid line shows the total opacity, which is the sum of the opacity from bound-free (dashed line), electron scattering (thin solid line), free-free (dotted line) and line expansion opacity (dot-dashed). The open circles are from the tabulation of the Opacity Project.

$$\tau_z = 7 \times 10^3\ \kappa_R \zeta_3^{-2} m_\star r_\star^{-2} \left(\frac{100}{E_z}\right)^{2/3} \left(\frac{E_t}{10}\right)^{1/3} \tag{18}$$

where $\zeta_3 = \zeta/10^3$ and κ_R is the Rosseland mean opacity in units of cm^2 g^{-1}. The debris is very optically thick for $\kappa_{\rm es} \approx 0.4$ cm^2 g^{-1}, the value for Thomson scattering in ionized hydrogen. However, the opacity drops dramatically with hydrogen recombination. From Eq. 12, the free electron density decreases by a factor $\sim \exp(-\epsilon_H/2k_BT) \sim 10^{-3}$ as the temperature changes from 10^4 K to 5000 K.

Other relevant sources of opacity likewise decline sharply for $T < 10^4$; free-free because of the declining electron density and bound-free because of the reduced occupation number of excited levels. The H^- and molecular opacities, however, may start to become more significant at lower temperatures. In addition, Doppler broadening in the differentially expanding debris enhances the line opacity from numerous iron group lines. In Figure 3 we plot the various sources of opacity as a function of temperature. The opacity reaches a minimum value of $\kappa_{\rm min} \approx 5 \times 10^{-4}$ cm^2 g^{-1} at $T \approx 5000$ K.

The unbound debris may thus begin to radiate effectively when the outermost layers of material have cooled to the "transparency" temperature $T_t \approx 5000$ K. This emission should begin at roughly a time $t_t = \zeta_R t_e$ after pericenter passage

$$t_t = 13\ \zeta_3 \beta^{-1} m_6^{-1/6} m_\star^{-1/3} r_\star^{3/2} \left(\frac{E_z E_t}{1000}\right)^{1/3}\ {\rm days} \tag{19}$$

Around this time, a sharp recombination front develops in the outer layers of debris − ionized material below the front is optically thick, while neutral material above will be optically thin if the densities are sufficiently low. Radiative cooling at the front promotes further recombination, causing this surface to move progressively inward in mass coordinates. The so-called transparency wave

(Zel'Dovich & Raizer 1967; Grasberg & Nadezhin 1976) allows for a more rapid release of the internal energy.

The condition for a transparency wave to successfully propagate is that the optical depth evaluated at the minimum opacity be of order unity. From Eq. 18 and $\kappa_{\rm min} = 5 \times 10^{-4}$ this occurs for expansion factors $\zeta \gtrsim 1500$. The thermodynamic evolution of §3 predicts expansion factors of $\zeta_R \sim 1000$ before recombination is complete. The coincidental near equality of these numbers indicates that it is possible, though just marginally so, for a recombination wave to occur and radiate away a significant fraction of the remaining internal energy.

The photosphere of the debris, which is coincident with the recombination front, cools by radiating a flux σT_t^4. Assuming that gas interior to the front is nearly neutral at a temperature near T_t, the speed at which transparency wave releases the internal energy and propagates inward is

$$v_{\rm tw} = \frac{\sigma T_t^4}{3/2 n k T_t} \approx 600\ \zeta_3^3 {m_\star}^{-1} {r_\star}^3 \left(\frac{T_t}{5000\ {\rm K}}\right)^3\ {\rm km\ s}^{-1} \tag{20}$$

The timescale for the light curve to decline after peak will be comparable to the time it takes the transparency wave to propagate the distance R_z

$$t_{\rm tw} = 1.3\, \zeta_3^{-2} m_\star {r_\star}^{-2} \left(\frac{100}{E_z}\right)^{2/3} \left(\frac{E_t}{10}\right)^{1/3} \left(\frac{T_t}{5000\ {\rm K}}\right)^{-3} {\rm days} \tag{21}$$

The luminosity of the light curve, as viewed perpendicular to the orbital plane, will be roughly that of a blackbody at T_t with the given projected surface area.

$$\begin{aligned} L &= 4\pi {R_\star}^2 \zeta^2 E_z^{2/3} E_t^{-1/3} \sigma T_t^4 \\ &\approx 2\times 10^{40}\ \zeta_3^2 {r_\star}^2 \left(\frac{E_z}{100}\right)^{2/3} \left(\frac{10}{E_t}\right)^{1/3} \left(\frac{T_t}{5000\ {\rm K}}\right)^4\ {\rm ergs\ s}^{-1} \end{aligned} \tag{22}$$

The disruption of solar mass stars should give rise to rather brief, dim transients, while those of more massive stars will be significantly brighter given their greater $R_\star$ and ζ_R.

5. LIGHT CURVES

A realistic calculation of the optical emission from tidal disruption would require a 3-dimensional coupled radiation-hydrodynamics simulation. Here we perform simple 1-D calculations to illustrate the approximate luminosity and duration of the light curves.

The hydrodynamic simulations of Brassart & Luminet (2008) show that shocks tend to homogenize the debris structure in the z-direction. We consider models of initially uniform temperature and density $\rho_\star = M_{\rm ej}/V$, where the ejected mass is $M_{\rm ej} = M_\star/2$ and the initial volume $V = 4\pi {R_\star}^3/3$. The initial energy is given by Eq. 9 with $f_E = 1$ or 2. To estimate the light curves for stars of different masses, we apply a simple mass-radius relation $R_\star/R_\odot = (M/M_\odot)^{0.8}$.

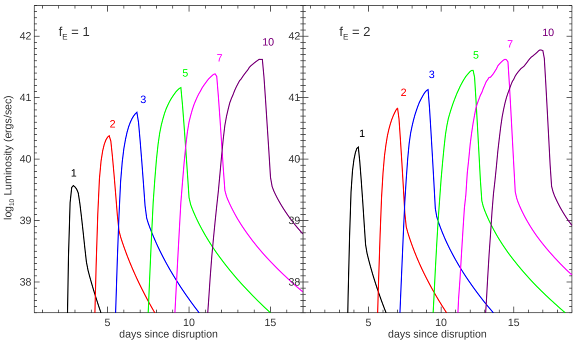

FIG. 4.— Bolometric light curves of recombination transients from the tidal disruption of stars with masses $M = 1, 2, 3, 5, 10$ and 20 $M_\odot$(from left to right, marked on figure). The calculations assume $M_b = 10^6\ M_\odot$, $\beta = 3, E_t = 10, E_z = 100$ and a viewing angle perpendicular to the orbital plane. The left and right panels show calculations for two different values of the initial internal energy (Eq. 9). The temperature and density structures of the debris were assumed homogeneous.

Radiation transport is most relevant along the z-direction, which we resolve with 1000 zones. The diffusion time is long in the ionized central regions, so radiation transport is only of critical importance in the surface layers. We therefore calculate the adiabatic evolution as described in §3 while including radiative losses relevant for the cooling recombination wave, namely

$$\dot{E}_{\rm rad} = e^{-\bar{\tau}_z} \delta t \kappa \rho c a T^4 \tag{23}$$

where δt is the duration of the timestep. The isotropic equivalent luminosity at a given time, as seen from the brightest viewing angle, is

$$L(t) = 4\pi {R_\star}^2 \zeta^2 E_z^{2/3} E_t^{-1/3} \sigma \int d\tau e^{-\tau} T^4(\tau) \tag{24}$$

where τ is the optical depth along the z-direction (Eq. 18). Given the small z-dimension, we neglect light crossing times.

Figure 4 shows light curves of disruption events for stars of masses $M = 1 - 10\ M_\odot$. We have taken a penetration factor of $\beta = 3$ and axis ratios $E_z = 100, E_t = 10$. As expected, the light curves rise at about 3 to 5 days after disruption, and last around a few days. Following the peak there is a more slowly declining light curve tail in which the neutral, cold ($T \sim 2000$ K) debris continues to radiate in the infrared. A proper description of the transport in this late phase would require inclusion of molecular opacities.

A solar mass star reaches a peak luminosity of 4×10^{39} ergs/sec for $f_E = 1$ and 2×10^{40} ergs/sec for $f_E = 2$. The brightnesses increases strongly with $M_\star$, mainly because the more massive stars have larger radii and hence greater surface area. In addition, more massive stars have initially larger internal energies and lower average densities, which allows for larger expansion factors (§3). The disruption of $M_\star > 10\ M_\odot$ stars, though presumably rare events, would produce quite luminous recombination transients, approaching the brightness of Type II supernovae ($\sim 10^{42}$ ergs/sec) although with much shorter durations.

The emission of the recombination transient will be anisotropic due to the asymmetry of the debris. To first order this angular dependence is given by the projected surface area of the photosphere along different viewing angles. For $E_z \gg 1$ the angular dependence is essentially $L \propto \cos(i)$, where i is the viewing angle relative to the

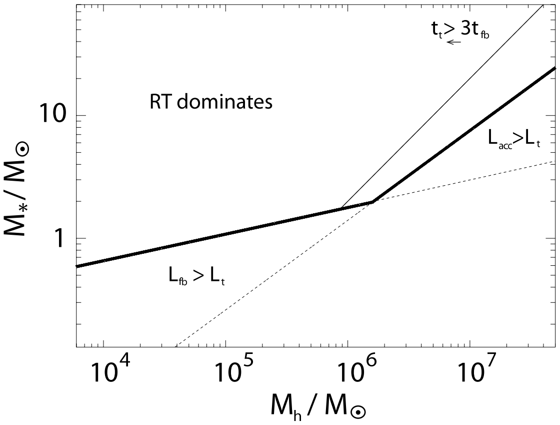

FIG. 5.— Domain in $M_\star$-$M_{\rm bh}$ space where the emission from the unbound debris exceeds the optical luminosity of accretion and fallback, as defined in the text. The recombination transient dominates in the region above the thick solid line (i.e., smaller black hole mass $M_{\rm bh}$ and larger stellar mass $M_\star$). The thin solid line shows the region where the time of peak for the recombination transient is comparable to the fallback timescale.

direction perpendicular to the orbital plane.

The spectrum of the recombination transient should be roughly blackbody at the transparency temperature $T_t \approx 5000$ K. The ongoing recombination may also lead to strong emission in H_α. Thus the RT will likely be brightest in the R-band. The spectral features should is some ways resemble those of Type II supernovae, with P-Cygni profiles. The observed Doppler shifts, however, should be significantly lower, corresponding to velocities $v_\infty/E_z \sim 600\ \beta$ km s^{-1}. Given the extreme asymmetry, high levels of continuum linear polarization, near the limit of $\sim 11\%$ in plane parallel electron scattering atmospheres (Chandrasekhar 1960) should be observed from some viewing angles.

6. PROSPECTS FOR DETECTION

6.1. *Domain of Astrophysical Relevance*

The recombination transient is just one of several sources of electromagnetic radiation in a tidal disruption event. An important question is whether the luminosity of the RT can compete with the other emission mechanisms, in particular the fallback of the bound stellar debris and its subsequent accretion onto the black hole.

The energy radiated during the fallback phase may dominate the luminosity at early times. The most tightly bound debris moves on an elliptical orbit with semimajor axis $a = \frac{1}{2}R_p(R_p/R_\star)$ and returns to pericenter on the orbital timescale $t_{\rm fb} = 2\pi(a^3/GM_{\rm bh})^{1/2}$, or

$$t_{\rm fb} \approx 40\ \beta^{-3} m_6^{1/2} {r_\star}^{3/2} m_*^{-1}\ {\rm days}, \tag{25}$$

with less bound material falling back continually thereafter. The streams of fallback material undergo collisions which, after a few orbital timescales, circularize the orbits at a radius $\sim 2R_p$ determined by total angular momentum conservation (Ramirez-Ruiz & Rosswog 2009). The final binding energy of this circular orbit is much less than the binding energy of the initially elliptical orbits. Assuming the energy difference is radiated with efficiency ϵ over a few orbital timescales, $\sim 3t_{\rm fb}$, the luminosity is would be

$$\begin{aligned} L_{\rm fb} &= \frac{1}{2}\frac{GM_{\rm bh}}{2R_p}\frac{M_\star}{2}\frac{1}{3t_{\rm fb}} \\ &\approx 4.6\times 10^{43}\ \beta^4\ \epsilon_{0.1} m_6^{1/6} {m_\star}^{7/3} {r_\star}^{-5/2}\ {\rm erg\ s^{-1}}. \end{aligned} \tag{26}$$

where $\epsilon_{0.1} = 0.1\epsilon$ is highly uncertain. Assuming the photosphere is near $2R_p$, the emission temperature is

$$T_{\rm fb} \sim 2.4\times 10^5\ \beta^{3/2} m_6^{-1/8} {m_\star}^{3/4} r_*^{-9/16}\ {\rm K}. \tag{27}$$

It is possible that some of the energy available in fallback goes into driving a mass outflow (Strubbe & Quataert 2009). This matter adiabatically expands to large radii until becoming optically thin. For certain choices of the fraction of mass ejected, the resulting optical luminosity can be quite bright $L \sim 10^{42} - 10^{43}$ ergs s^{-1}.

After circularization, the fallback material forms a torus which will spread out viscously and accrete onto the black hole. The timescale for this stage of the evolution is determined by the viscous timescale (Cannizzo et al. 1990; Ulmer 1999)

$$t_{\rm acc} \sim 73\left(\frac{\alpha}{0.1}\right)^{-1}\left(\frac{h}{0.1}\right)^{-2} {m_\star}^{-1/2} {r_\star}^{3/2}\ {\rm days}. \tag{28}$$

where α is the standard viscosity parameter (Shakura & Sunyaev 1973), and h is the ratio of the disk height to radius and is approximately of order unity for thick disks. The emergent radiation may have a strong dependence on the structure and orientation of the disk. As a simple estimate we consider the luminosity to be at the Eddington limit $L_{\rm ed} \approx 10^{44}\ m_6$ ergs s^{-1} and emanating from the radius $2R_p$. This gives an accretion temperature

$$T_{\rm acc} \sim 1.6\times 10^5\ \beta^{1/2} m_6^{1/12} {m_\star}^{1/6} {r_\star}^{-1/2}\ {\rm K}. \tag{29}$$

Both the fallback and the accretion temperature depend weakly on $M_{\rm bh}$. In the case where emission peaks in the soft x-rays, we will observe in the optical the Raleigh-Jeans tail of the blackbody, where the flux is reduced by a factor $(T_{\rm fb}/T_t)^{-2}$ from its peak value.

From the above discussion, we can estimate the conditions under which the recombination transient is a relevant source of emission. Using Eq. 24 and assuming a simple mass-radius relation $r_\star = {m_\star}^{0.8}$, we find that the optical luminosity of the RT exceeds that of fallback and accretion, respectively, when the mass of the disrupted star exceeds

$$\begin{aligned} m_\star &\gtrsim\ 1.8\ (\beta/3)^{15/28} \epsilon_{0.1}^{15/28} m_6^{25/112} \\ \text{for } L_{\rm t} &\gtrsim L_{\rm fb}(T_{\rm fb}/5000\ {\rm K})^{-2} \end{aligned} \tag{30}$$

and

$$\begin{aligned} m_\star &\gtrsim\ 1.4\ (\beta/3)^{-15/17} m_6^{25/34} \\ \text{for } L_{\rm t} &\gtrsim L_{\rm acc}(T_{\rm acc}/5000\ {\rm K})^{-2} \end{aligned} \tag{31}$$

Figure 5 depicts the relevant $M_\star$-$M_{\rm h}$ domain where the RT is likely to contribute significantly to the optical luminosity. While these estimates are subject to several uncertainties, it appears that the RT of $m_\star \approx 1$ disruptions will be most relevant when $M_{\rm bh} < 10^6\ M_\odot$. For more massive black holes, disruption of larger stars may be necessary. The RT appears to be comparable to or brighter than the optical emission resulting from the reprocessing of x-rays in the unbound debris, studied by Strubbe & Quataert (2009). However, if the super-Eddington outflows also discussed by Strubbe & Quataert (2009) occur, their optical luminosity can, for certain wind parameters, be as high as $\sim 10^{42} - 10^{43}$ ergs, which would completely dominate the RT of even massive stars, at least at early times.

Even if the RT luminosity falls below the other sources, it may be discernible if it is separated in time. From Eq. 19, the ratio of the RT timescale, t_t to the accretion/fallback timescales, $\sim 3t_{\rm fb}$, is

$$\frac{t_{\rm t}}{3t_{\rm fb}} \sim 0.1\ \beta^2 m_6^{-2/3} {m_\star}^{2/3}. \quad (32)$$

Thus for black holes $M_{\rm bh} > 10^6\ M_\odot$ the RT might be observable as a precursor to the black hole accretion and fallback signatures (Figure 5). In this case it may serve as a confirming signature that the event being witnessed is in fact a tidal disruption event.

The detection of disruption transients also requires that the optical emission reach some significant fraction of the luminosity of the host galaxy nucleus. At a distance of 400 Mpc, ground based optical surveys with a resolution of a ~ 1" will only resolve a kiloparsec-sized bulge. McLure & Dunlop (2002) give a empirical correlation between bulge luminosity L_b and central black hole mass. For $M_{\rm bh} = 10^8\ M_\odot$, the bulge luminosity $L_b \approx 2 \times 10^9\ L_\odot$, and only the disruption of $\gtrsim 10\ M_\odot$ stars could contribute $\gtrsim 10\%$ of the core brightness for galaxies. For $M_{\rm bh} \lesssim 10^7\ M_\odot$, on the other hand, the disruption of $m_\star > 3$ stars would outshine the galaxy and be easily detectable. However, firm evidence for the assumed $M_{\rm bh} - L_b$ correlation below $M_{\rm bh} < 10^7 M_\odot$ is still lacking.

6.2. *Detection Rates*

Observational surveys are being designed which will probe the magnitude range ($M_{\rm bol} = -11$ to -14) of the recombination transients. LSST, for example, will reach an R-band magnitude of $M_R = 24$ mag per shot. In this case, a $M = 1\ M_\odot$ disruption would be detectable out to ~ 100 Mpc, the distance to the Coma cluster, while an $M = 10\ M_\odot$ disruption would be detectable much further out, to $z \approx 0.1$.

Wang & Merritt (2004) derived a total disruption rate for early-type galaxies and bulges by combining an expression for the disruption rate

$$\dot{N} \approx 2.2 \times 10^{-4}\ {\rm yr}^{-1}\ h^{-0.25} (L_g/10^{10} h^{-2} L_\odot)^{-0.295} \quad (33)$$

with Ferguson & Sandage (1991) E+SO luminosity function for the galaxy luminosities L_g. They found a rate per unit volume of $\sim 10^{-5}\ {\rm yr}^{-1}\ {\rm Mpc}^{-3}$, with galaxies with $L_g \leq 10^9 L_\odot$ ($M_{\rm bh} \leq 10^8 M_\odot$) dominating the consumption rate. Assuming that galaxies with $L_g \ll 10^9 L_\odot$ hosting black holes are at least as common, we estimate that LSST may detect RTs of more massive stars at a rate of $\geq 300 \psi_{>5}\ {\rm yr}^{-1}$, where $\psi_{>5}$ is the fraction of total disruptions of stars with $m_* \geq 5$.

The major uncertainty in this rate is whether low luminosity galaxies contain a nuclear black hole, as M32 is currently the faintest system ($L_g \sim 4 \times 10^8 L_\odot$) for which there is solid kinematical evidence. The galaxies in question are dwarf elliptical (dE) galaxies, which are the most numerous type of galaxy in the Universe. Tidal disruption events are also more common in dE galaxies, and if they contain nuclear black holes they should dominate the total tidal flaring rate. Assuming that only nucleated dE galaxies (dEn) contain black holes, Wang & Merritt (2004) found a total tidal disruption for dEn in Virgo of $\sim 0.2\ {\rm yr}^{-1}$. The overall rates in the Coma Cluster are expected to be significantly larger. These event rates will be even higher if moderately massive black holes are present in every dE galaxy or in bulges of late-type spirals.

Suggestive evidence has accumulated that intermediate mass black holes ($M_{\rm bh} = 10^3 - 10^4\ M_\odot$) exist in some globular clusters (e.g. Noyola et al. 2008). The rate of tidal disruption events in these systems is expected to be $\sim 10^{-7}\ {\rm yr}^{-1}$ per globular cluster (Baumgardt et al. 2004). Taking a globular cluster space density of $n_{\rm gc} \sim 4\ {\rm Mpc}^{-3}$ (Brodie & Strader 2006) we estimate the density rate of RT to be at most $\sim 4 \times 10^{-7} {\rm yr}^{-1}\ {\rm Mpc}^{-3}$. In this case, LSST should detect RT events arising from the disruption of a 1 $M_\odot$ star with a rate of $\sim 5\psi_{>1} {\rm yr}^{-1}$. The globular cluster luminosity function in the galaxies studied to date (Brodie & Strader 2006) is well fit by a Gaussian distribution with a peak $M_V \sim -7.4$ and $\sigma \sim 1.4$. The RT should thus easily outshine the cluster's optical luminosity. Non-detection of flares after a few years would argue against the existence of intermediate mass black holes in globular clusters.

7. SUMMARY AND CONCLUSIONS

The purpose of this paper is has been to explore whether the unbound debris of tidal disruption might give rise to luminous optical emission, and to determine under what conditions this emission may be observationally relevant. The analytical results predict a brief (3-5 day) optical transient with peak luminosities in the range $2 \times 10^{40} (M_*/M_\odot)^{5/2}$ ergs s^{-1}. The energy for the emission is stored mostly in the ionization energy of hydrogen, and is released when the ejecta becomes neutral and transparent at temperatures $T \approx 5000$ K. This physics will be relevant not only for the tidal disruption of stars by massive black holes, but to the weak ejection of hydrogen envelopes in general by, e.g., stellar collisions or pulsations.

The predicted bolometric luminosities of the recombination transients fall into the interesting – that is to say, relatively unexplored – range between novae and supernovae. Upcoming synoptic surveys will begin to probe these sorts of intermediate events. The RT of 1 $M_\odot$ stars are relatively dim events which would only be visible in the nearby universe (~ 100 Mpc). The disruption of more massive stars ($M \gtrsim 5\ M_\odot$), on the other hand, can be quite bright. Such events may not be as rare as one might first expect. There is strong evidence that the initial mass function of stars within the Galactic center is top heavy (Alexander 2005). Perhaps massive stars are more common in the cores of other galaxies as well.

For massive black holes, $M_{\rm bh} > 10^6\ M_\odot$, the optical luminosity from the accretion of bound material likely surpasses the emission from the unbound debris. Nevertheless, the RT may still be discernible as a precursor, and may provide a important complementary signature. While the properties of the accretion flare depends most sensitively on the black hole mass, the luminosity of the RT depends primarily on the properties of the disrupted star, with little dependence on $M_{\rm bh}$. In principle observations of both components would allow one to solve for the parameters of the event, providing insight into both the black hole mass and stellar population in the centers of distant galaxies. More basically, detection of a RT would provide confirmation that the event witnessed was in fact a legitimate tidal disruption,

Recombination transients appear to be of greatest interest for probing lower mass black holes ($M_{\rm h} < 10^6 M_\odot$). In these systems, the optical luminosity of the transient is likely to exceed that of accretion, and should outshine the nucleus of the galaxy. This offers one means of searching for low mass black holes in dwarf galaxies, or for intermediate mass black hole in globular clusters. If black holes do lurk in these numerous locations, the recombination transient might be the most prominent optical signature of a stellar disruption.

We thank J. Bloom, S. Gezari, J. Guillochon, E. Quataert, X. Prochaska, S. Rosswog, Martin Rees, L. Strubbe, and the referee for useful discussions and comments. Support for DK was provided by NASA through Hubble fellowship grant #HST-HF-01208.01-A awarded by the Space Telescope Science Institute, which is operated by the Association of Universities for Research in Astronomy, Inc., for NASA, under contract NAS 5-26555. This research has been supported by the DOE SciDAC Program (DE-FC02-06ER41438). ER acknowledge support from the David and Lucile Packard Foundation.

REFERENCES

Alexander, T. 2005, Phys. Rep., 419, 65
Baumgardt, H., Makino, J., & Ebisuzaki, T. 2004, ApJ, 613, 1143
Bogdanović, T., Eracleous, M., Mahadevan, S., Sigurdsson, S., & Laguna, P. 2004, ApJ, 610, 707
Brassart, M., & Luminet, J.-P. 2008, A&A, 481, 259
Brodie, J. P., & Strader, J. 2006, ARA&A, 44, 193
Cannizzo, J. K., Lee, H. M., & Goodman, J. 1990, ApJ, 351, 38
Carter, B., & Luminet, J.-P. 1983, A&A, 121, 97
Chandrasekhar, S. 1960, Radiative Transfer (New York: Dover, 1960)
Donley, J. L., Brandt, W. N., Eracleous, M., & Boller, T. 2002, AJ, 124, 1308
Esquej, P., Saxton, R. D., Freyberg, M. J., Read, A. M., Altieri, B., Sanchez-Portal, M., & Hasinger, G. 2007, A&A, 462, L49
Ferguson, H. C., & Sandage, A. 1991, AJ, 101, 765
Gezari, S. et al. 2009, ApJ, 698, 1367
—. 2006, ApJ, 653, L25
Grasberg, E. K., & Nadezhin, D. K. 1976, Ap&SS, 44, 409
Guillochon, J., Ramirez-Ruiz, E., Rosswog, S., & Kasen, D. 2008, ArXiv e-prints
Khokhlov, A., & Melia, F. 1996, ApJ, 457, L61+
Kim, S. S., Park, M.-G., & Lee, H. M. 1999, ApJ, 519, 647
Kobayashi, S., Laguna, P., Phinney, E. S., & Mészáros, P. 2004, ApJ, 615, 855
Kochanek, C. S. 1994, ApJ, 422, 508
Krishna Swamy, K. S. 1961, ApJ, 134, 1017
Lodato, G., King, A. R., & Pringle, J. E. 2009, MNRAS, 392, 332
McLure, R. J., & Dunlop, J. S. 2002, MNRAS, 331, 795
Mihalas, D., & Weibel Mihalas, B. 1984, Foundations of radiation hydrodynamics
Noyola, E., Gebhardt, K., & Bergmann, M. 2008, ApJ, 676, 1008
Ramirez-Ruiz, E., & Rosswog, S. 2009, ApJ, 697, L77
Rees, M. J. 1988, Nature, 333, 523
Rosswog, S., Ramirez-Ruiz, E., & Hix, W. R. 2009, ApJ, 695, 404
Shakura, N. I., & Sunyaev, R. A. 1973, A&A, 24, 337
Strubbe, L. E., & Quataert, E. 2009, ArXiv e-prints
Ulmer, A. 1999, ApJ, 514, 180
Wang, J., & Merritt, D. 2004, ApJ, 600, 149
Zel'Dovich, Y. B., & Raizer, Y. P. 1967, Physics of shock waves and high-temperature hydrodynamic phenomena